The Seepage Behavior of a High Concrete Face Rockfill Dam on Alluvium Deposit

Weijun Cen[1], Dengjun Li[1], Erich Bauer[2]

1- College of Water Conservancy & Hydropower Engineering, Hohai University, Nanjing, China
2- Institute of Applied Mechanics, Graz University of Technology, Graz, Austria

Email: hhucwj@163.com

Abstract

The nodal virtual flux method with a fixed finite element mesh is employed to investigate the non-confined seepage field of a high concrete face rockfill dam on an alluvium deposit layer after water impounding. Particular attention is also paid to the change of the seepage behavior caused by a local defect of the anti-seepage system located at the upstream side of the dam. The anti-seepage system considered consists of concrete face slabs, toe slabs connected with the grouting curtain in the dam foundation, and the seal system of the joints between the concrete slabs. For the intact anti-seepage system, the numerical results indicate that the seepage field is mainly concentrated in the dam foundation, and the location of the phreatic surface in the dam body is very low under normal conditions. Once a crack in the slab or a local failure of the concrete joint seal occurs the seepage behavior of the dam changes significantly. The concrete face slabs, joint seal and the sufficient depth of the grouting curtain are the significant anti-seepage barriers to control the seepage behavior of the dam, and particular attention should thus be paid to these elements for the design and construction of concrete face rockfill dams.

Keywords: CFRD, Alluvium Deposit, Seepage Behavior, Anti-Seepage System.

1. INTRODUCTION

The development of enhanced concepts for the construction of concrete face rockfill dams (CFRDs) started after the completion of Cethana CFRD in the 1960s. In China the application of modern construction concepts for CFRDs began relatively late, but over the past few decades, development has been very fast. Starting from one of China's first CFRD with a height of 95 m (begun in 1985 and completed in 1990 at Xibeikou) to the Shuibuya CFRD with a height of 233 m (completed in 2008), the number and height of Chinese CFRDs have made significant progress and has become one of the most competitive dam types in dam design, e.g. [1]. So far, there are approximately 40 CFRDs with heights of over 100 m. In the near future the height of CFRDs to be constructed such as the one in Rumei and Gushui will reach or exceed a height of 300 m. The safety of CFRDs can be strongly influenced by defects of the anti-seepage measures, which can lead to local erosion, collapse settlement and large creep deformation [2, 3]. In this context particular attention should already be paid in the design phase to the investigation of seepage fields under different scenarios. In the anti-seepage measures context, the CFRD is entirely different from the traditional earth-rock dam with a core wall. The anti-seepage system of a CFRD consists of the upstream concrete face slab, toe slab, joint seal and wave wall. As discussed in the present paper for a CFRD on an alluvium deposit, the grouting curtain or cut-off wall connecting with the toe slab is also needed to form a closed seepage control system. In particular, in the present paper a 138 m high CFRD located in Sichuan Province in China is considered for analyzing the seepage field in the CFRD and foundation under different boundary conditions. The investigations mainly focus on factors and scenarios affecting the seepage behavior such as the occurrence of cracks in concrete slabs, the permeability of cushion layers, the design depth of the curtain, and the permeability of the foundation. The location of the phreatic surface is computed using the virtual flux method for a finite element mesh fixed in space. The conclusions that can be drawn from the results of the present analysis may provide a useful reference for the design of CFRDs.

2. BASICS FOR MODELLING THREE-DIMENSIONAL SEEPAGE FIELDS

2.1. GOVERNING EQUATIONS AND BOUNDARY CONDITIONS

With respect to Darcy's law and the continuity condition for fluid flow through an anisotropic porous media, the governing equations of the three-dimensional steady-state seepage can be written as [4, 5]:

$$-\frac{\partial}{\partial x_i}(k_{ij}\frac{\partial h}{\partial x_j})+Q=0 \tag{1}$$

where x_i denotes the *i* coordinate (*i*=1,2,3); k_{ij} is coefficient tensor of permeability; the hydraulic head $h=x_3+p/\gamma$ is the sum of the elevation x_3 and the pressure had p/γ; and Q is the source or sink term.
The corresponding boundary conditions are as follows:

$$h|_{\Gamma_1}=h_1 \tag{2}$$

$$-k_{ij}\frac{\partial h}{\partial x_j}n_i|_{\Gamma_2}=q_n \tag{3}$$

$$-k_{ij}\frac{\partial h}{\partial x_j}n_i|_{\Gamma_3}=0,\ h=x_3 \tag{4}$$

$$-k_{ij}\frac{\partial h}{\partial x_j}n_i|_{\Gamma_4}\geq 0,\ h=x_3 \tag{5}$$

where h_1 is the known hydraulic head; n_i is the exterior normal direction cosine of the seepage boundary surface, (*i*=1, 2, 3); Γ_1, Γ_2, Γ_3 and Γ_4 are the Dirichlet boundary, the Neumann boundary, the boundary of the free seepage surface, and the boundary of the seepage exit face, respectively; q_n is the normal flow, in which the sign of outflow is positive.

2.2. THE NODAL VIRTUAL FLUX PROCEDURE FOR A FIXED FINITE ELEMENT MESH

According to the variational principle, Eqs. (1)-(5) are equivalent to the following equations [6, 7]:

$$\prod(h)=\frac{1}{2}\int_{\Omega_1}k_{ij}\frac{\partial h}{\partial x_i}\frac{\partial h}{\partial x_j}d\Omega. \tag{6}$$

$$[K_1]\{h_1\}=\{Q_1\} \tag{7}$$

where $[K_1]$ is the conduction matrix of the seepage in real domain, $\{h_1\}$ is the nodal head array and $\{Q_1\}$ is the equivalent nodal flow array.

For unconfined seepage problems, the free surface of the seepage domain can be computed with help of the nodal virtual flux method. The corresponding iteration formula reads [8]:

$$[K]\{h\}=\{Q\}-\{Q_2\}+\{\Delta Q\} \tag{8}$$

where $[K]$ is the conduction matrix of total computational domain $\Omega=\Omega_1+\Omega_2$; $\{h\}$ is the nodal head array; $\{Q\}$ is the equivalent nodal flow array. Ω_1 and Ω_2 are the real seepage domain and the virtual domain, respectively. The two domains are divided by the free seepage surface in seepage field Γ_3. $\{Q_2\}$ is the equivalent nodal flow array in the virtual domain Ω_2. The array $\{\Delta Q\}=[K_2]\{h\}$ denotes the virtual flux of the nodes of the virtual elements and transitional elements in the virtual seepage domain Ω_2. The so-called transition elements are located in the virtual domain and crossed by the free water table Γ_3 [9].

2.3. LOCAL SEEPAGE BEHAVIOR IN CRACKS OF THE CONCRETE FACE SLABS AND LEAKING OF THE SEALING JOINTS

The analysis of CFRDs shows, that the concrete face slabs in the central riverbed are compressed, while the slabs near the abutments are pulled in the direction of the dam axial. The slabs on the top and bottom are also pulled, while in the central area the labs are compressed along the dam slope. Based on the deformation characteristics of the entire structure, horizontal cracks can appear in the central part, and tensile cracks can appear near the abutments [8]. Because the concrete face slabs and toe slabs are connected to each other by joints, it can happen that the sealing will be pulled out in the peripheral joints close to the bottom and joints near the abutments will be opened. Once such defects occur, the seepage behavior changes significantly. In finite element simulations, thin-layer elements can be used to reflect the corresponding seepage behavior of cracks. To generate thin-layer elements a very fine discretization of the mesh is needed. In this context, however, the selection of the element thickness and equivalent hydraulic conductivity are generally based on experience. In this paper, the plane joint element with zero thickness is used for the simulation of cracks or joints instead of thin-layer element [11, 12]. The local seepage behaviors due to cracks in concrete slabs or leakage of joint sealing can be described by the following relation [13]:

$$v_f = k_f J_f = \frac{g b_f^2}{12\mu} J_f \tag{9}$$

where v_f, k_f, J_f are the average velocity within the joint, the equivalent hydraulic conductivity and hydraulic gradient respectively, b_f is the width of the cracks or joints, μ is the viscosity coefficient of water, and g is acceleration of gravity. The flow in plane cracks or joints can be written as:

$$-\frac{\partial}{\partial x_i^f}(k_{ij}^f \frac{\partial h}{\partial x_j^f}) = 0 \quad (i, j = 1, 2) \tag{10}$$

where k_{ij}^f is the coefficient tensor of permeability in the joint element; x_i^f is the local coordinate of the joint element.

3. CASE STUDY

3.1. GEOTECHNICAL CONDITIONS AND MATERIAL PARAMETERS

In this study a 138 m high CFRD located in Sichuan Province in China is considered. The dam height is 138 m. The crest width is 10 m and the length of dam axis is 292 m. Both upstream and downstream slope ratios are 1:1.4. The consolidation grouting depth under the toe slab is 10 m and the maximum depth of grouting curtain is 75 m. The typical cross section of the CFRD is shown in Figure 1. According to the geologic conditions and the dam profiles, a 3D finite element mesh is used to analyze the seepage field for the dam on alluvium deposit. The FE model is discretized by 36619 nodes and 34156 solid elements in form of hexahedra, prism or tetrahedral (Figure 2). A part of the mesh of the anti-seepage system is illustrated in Figure 3.

According to the laboratory experiments carried out with the dam materials, the coefficients of permeability of cushion layer (2A), special cushion layer (2B), transitional layer, main and secondary rockfill zones, filter layer, alluvium deposit layer are taken as 2.10×10^{-4} cm/s, 1.00×10^{-4} cm/s, 3.17×10^{-3} cm/s, 3.40×10^{-1} cm/s, 6.62×10^{-1} cm/s, 1.00×10^{-3} cm/s and 7.2×10^{-1} cm/s, respectively. The coefficients of permeability of face slab, toe slab and grouting curtain are taken as 1.00×10-7 cm/s and 3.00×10-5 cm/s, respectively. The coefficients of permeability of rock foundation above 10 Lu, between 10 Lu and 3 Lu, and less than 3 Lu are 1.00×10-3 cm/s, 2×10-4 cm/s and 3×10-5 cm/s, respectively.

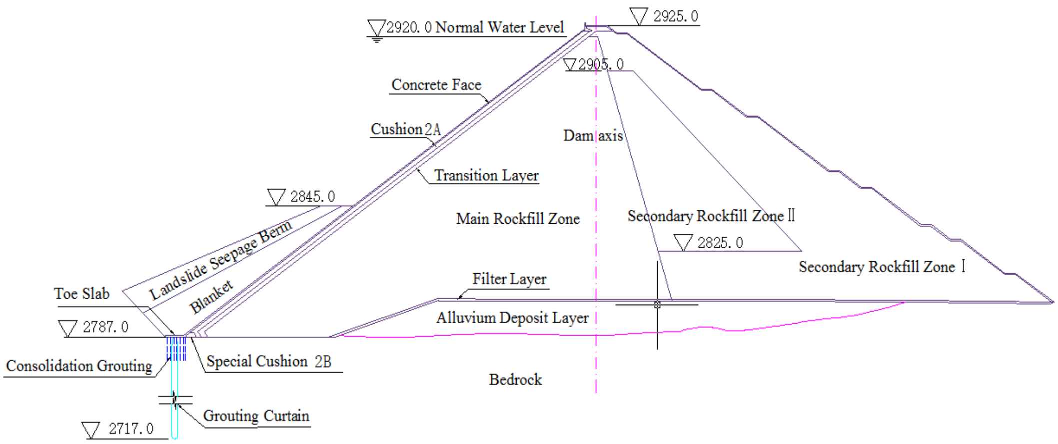

Figure 1. Cross section of the CFRD considered in the present study.

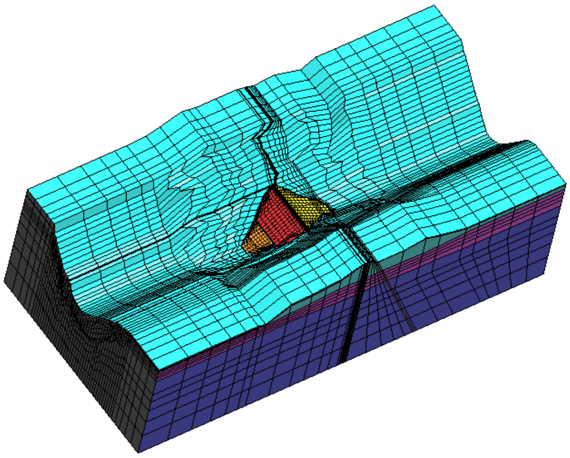

Figure 2. Finite element mesh of dam and foundation.

To investigate the relevance of the seepage control system under different working conditions and for reasonable local failure events numerical simulations were carried out with respect to different upstream and downstream water levels, reasonable cracking events in concrete slabs and local failure of the joint sealing, the depth of the grouting curtain, and the permeability's of the cushion layer and the bedrock.

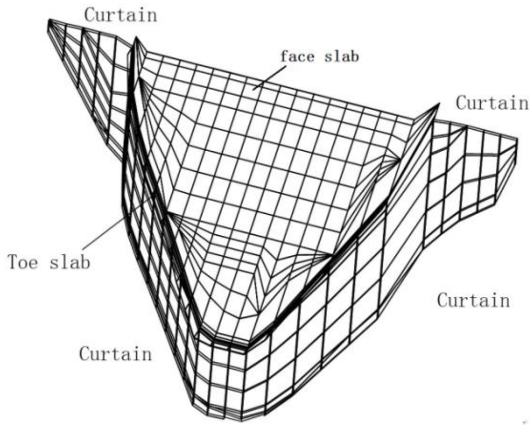

Figure 3. Finite element mesh of the anti-seepage system.

3.2. SIMULATION OF SEEPAGE BEHAVIOR OF THE DAM AND FOUNDATION FOR THE INTACT ANTI-SEEPAGE SYSTEM

In order to investigate whether specific anti-seepage measures are needed, the natural seepage behavior of the dam foundation is first analyzed. Numerical simulations show that for the existing geological condition and a water level of 2920 m in the reservoir, the total seepage flux will increase from 11414.6 m3/day (calculated for the CFRD with intact grouting curtain) to 26968.9 m3/day for the CFRD without grouting curtain. Thus, the flux of the dam foundation is doubled.

The seepage characteristics are significantly different in the left and right abutments. In particular, the seepage flow through the left abutment is about 59% of the total flux. If the coefficients of permeability of the dam foundation and alluvium deposit are assumed to increase by 30%, the flux increases up to approximately 24%. This indicates that the seepage occurs mainly in the dam foundation, thus suitable anti-seepage measures should be taken in the foundation.

For the intact seepage control-system with the grouting curtain the distribution of the total water head of dam and foundation at normal water level of 2920 m is shown in Figure 4. Higher gradients of the isolines can be detected mainly in the dam foundation. The phreatic surface in the dam body is located only a little higher than the downstream water level. The gradient of the isolines in the grouting curtain indicates that the curtain plays a key role in controlling the seepage field in the dam foundation. There are great differences for the leakage flow through the dam body, the river bed and for the left and right abutments of the mountain which comprise 10%, 5%, 51% and 34% of the total seepage flux, respectively. From these together the total seepage flux through dam foundation and abutments is about 90%. This demonstrates the importance of seepage control measures for CFRDs in dam foundation and abutments despite the fact that the concrete face is in intact condition.

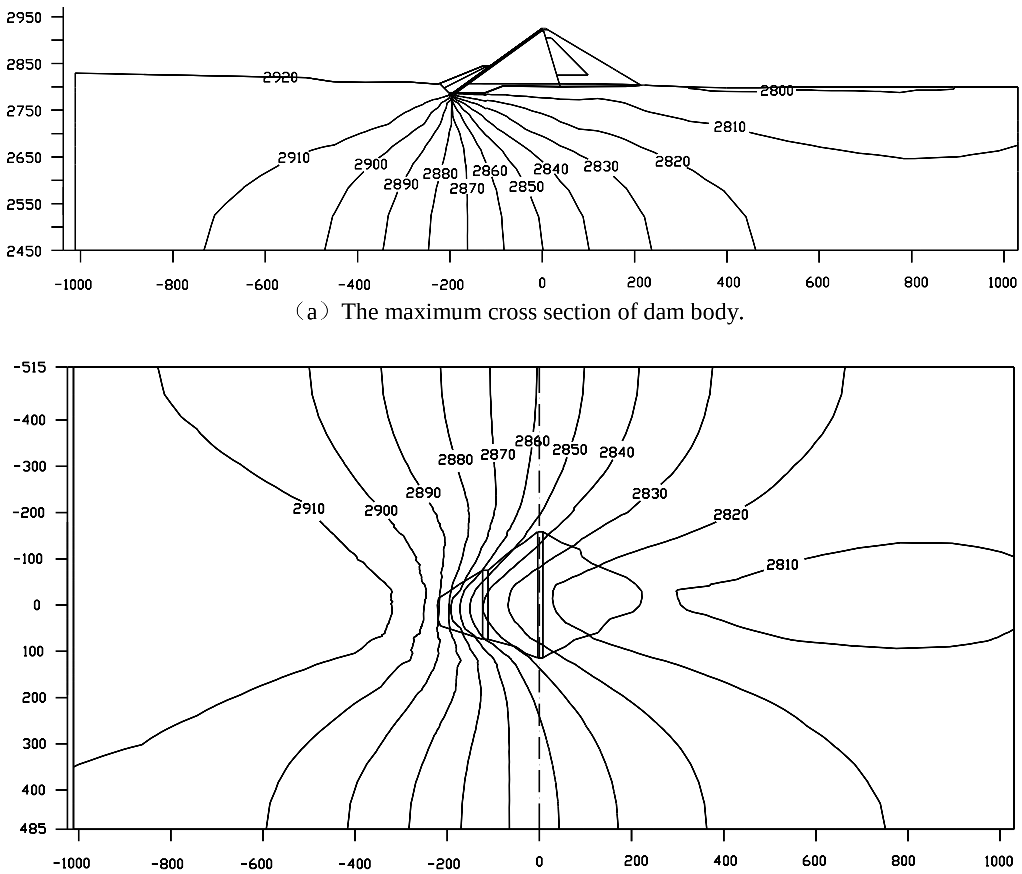

(b) Horizontal section of dam foundation at an elevation of 2730 m.

Figure 4. Isolines of the dam and foundation at normal water level of 2920 m in the reservoir (Unit: m)

3.3. SEEPAGE BEHAVIOR WITH LOCAL DEFECTS OF THE ANTI-SEEPAGE SYSTEM

Assume that the concrete face slab in the central riverbed is crushed along the vertical joint, water from the reservoir will flow through the crack into the dam body. As a consequence, the phreatic surface behind the crack will rise significantly. If the crack is assumed to be 1 mm wide and 1 m long the seepage flux will increase from 11414.6 m^3/day to 17707.5 m^3/day. Assume that the sealing of peripheral joints in the riverbed are in failure with a length of 1 m, the water head distribution of the seepage field changes only slightly and the increase of leakage flux does not exceed 5%. This is due to the low permeability of the special cushion layer. By contrast the cracking of face slabs and defects of the joint sealing above the special cushion has a much greater impact on both water head distribution and leakage flux of the seepage field. It is thus necessary to pay more attention to the seepage control design of these parts of the anti-seepage system. In addition, the sensitivity analysis of seepage flux of the concrete grouting curtain depth under normal design conditions shows that a good impermeable effect can be achieved as long as the curtain stretches between 1m and 2m below the 3Lu line of the rock foundation batholith zone.

3.4. SEEPAGE GRADIENT

The seepage gradients are large in the concrete face slab and concrete grouting curtain, but the values do not reach the permissible value for concrete.

Under normal conditions, the seepage failure will not occur in the transition layer, and the main rockfill zone for small seepage gradients. The secondary rockfill is almost in the dry zone and the maximum value of the seepage gradient is less than 0.001. Under normal working conditions the seepage gradients of the local cushion layer (2A) and special cushion layer (2B) reach 0.95 and 1.67 respectively.

If a face slab cracks or the seal ruptures, the cushion layer (2A) and special cushion layer (2B) can easily be destroyed due to an enormous increase of the seepage gradient. For the alluvium deposit the maximum value of the seepage gradient is less than 0.083 and thus, a seepage failure will not occur under the intact anti-seepage system. But if the grouting curtain is too short, the seepage gradient will increase to 0.201 and it is then possible that seepage failure may occur in zones with a gradient higher than the critical value. This also confirms the importance of appropriate installation of the grouting curtain.

3.5. SENSITIVITY ANALYSIS OF THE PERMEABILITY OF CUSHION LAYERS

If a crack in the concrete slab or a local failure of the joint sealing appears, the cushion layer (2A) and special cushion layer (2B) will function as seepage prevention due to their low permeability. In the design of CFRDs, this functionality is referred to as an auxiliary anti-seepage role. An analysis of the sensitivity of the permeability of the cushion layer (2A) was carried out for two different assumed coefficients of permeability and the results are compared with the original design value of 2.1×10^{-4}cm/s. The computed results show that the seepage gradients of the cushion layer reduce to 0.37 and 0.14 for a permeability of 7.1×10^{-4}cm/s and 2.1×10^{-3}cm/s, respectively. The distribution of isolines of the water head and the total seepage flux show no significant changes. It can be concluded that for the effective auxiliary seepage control measure, the semi-permeability of the cushion layer should between 10^{-3} to 10^{-4} cm/s. In addition, the construction quality of the cushion layer (2A), the special cushion layer (2B) and the transition layer is also important to increase the required capacity of the auxiliary anti-seepage measure.

4. CONCLUSIONS

(1) The sensitivity analysis shows that the coefficient of permeability of the bedrock and alluvium deposit have a great influence on the total seepage flux because the seepage field is mainly concentrated in the dam foundation.

(2) The concrete grouting curtain strongly affects the seepage field in the foundation. In order to make sure that the work performance meets the design requirements, a sufficient depth of the curtain and also the quality of implementation is of importance.

(3) Cracks in the concrete slabs and local leakage in the joint sealing leads to a rising of the phreatic surface and to a significant increase of seepage flux in the dam body.

(4) If the coefficient of permeability of the cushion layer is too low, the seepage gradient in this zone will exceed the permissible value and can lead to seepage failure caused by internal erosion of the filling material. An appropriate higher permeability of the cushion layer will significantly reduce the seepage gradient, despite the fact that the dam leakage remains unchanged. Therefore, proper seepage properties of the cushion layer must be chosen in the design state of the CFRD to avoid seepage failure as a result of local imperfections in the seepage control system.

(5) An intact concrete slab and joint seal system as also the effective operation of the underground concrete grouting system is of great importance in seepage control. For the intact anti-seepage system, the seepage field is mainly concentrated in the dam foundation and the greater part of the dam is in an almost dry or a moist state.

5. REFERENCES

1. Li, N.H. (2007), "*New Technologies of High Concrete Face Rockfill Dam*", Beiijing, China Water and Power Press (in Chinese).
2. Alonso, E.E., Cardoso, R. (2010), "*Behavior of materials for earth and rockfill dams: perspective from unsaturated soil mechanics*", Frontier of Architecture and Civil Engineering in China, 4(1), pp. 1-39.
3. Bauer, E. (2009), "*Hypoplastic modeling of moisture-sensitive weathered rockfill materials*", Acta Geotechnica, 4, pp. 261-272.
4. Neuman, S.P. (1973), "*Saturated-unsaturated Seepage by Finite Elements*", ASCE, Journal of Hydraulic Division, pp. 2233-2250.
5. Neuman, S.P., Narasimhan, T.N, Witherspoon, P.A. (1977), "*Application of mixed explicit-implicit finite element method to nonlinear diffusion-type problems*", Finite Elements in Water Resources, Pentech Press, London, Plymouth.
6. Chen, S., Zhang, X. (2016), "*Seepage Control in a High Concrete Face-Rock Fill Dam Based on the Node Virtual Flow Method*", The Open Construction and Building Technology Journal, 10(1), pp. 547-560.
7. Zhu, Y.M., Gong D.Y. (2003), "*Solution to 3-D Unsteady Saturated-unsaturated Seepage Problem and Accurate Treatment of Saturated and Unsaturated Exit Surfaces of Seepage*", Advances in Water Science, 14(1), pp. 67-71, (in Chinese).
8. Zhu, Y.M., Wang, R.Y., Xu, H.B. (1992), "*Some Techniques for Solution to Free Surface Seepage Flow through Arch Dam Abutments*", In Proc. of the International Symposium on Arch Dams, Nanjing, China.
9. Zhu, Y.M., Sun, D., Bauer, E., Semprich, S. (2006), "*On refined FEM solution to seepage in arch dam foundation*", In Rock Mechanics in Underground Construction: ISRM International Symposium 2006: 4th Asian Rock Mechanics Symposium, 8-10 November 2006, Singapore (p. 441). World Scientific.
10. Cen, W.J., Wen, L.S., Zhang, Z.Q. (2016), "*Numerical simulation of seismic damage and cracking of concrete slabs of high concrete face rockfill dams*", Water Science and Engineering, 9(3), pp. 205-211.
11. Goodman, R. E., Taylor, R.L., Brekke, T.L. (1968), "*A model for the mechanics of jointed rock*", Journal of Soil Mechanics & Foundations Div., 94, pp. 637-660.
12. Chowdhury, S.R, Narasimhan, R. (2000), "*A cohesive finite element formulation for modelling fracture and delamination in solids*", Sādhanā, 25(6), pp. 561-587.
13. Wittke, W. (1984), "*Felsmechanik-Grundlagen für wirtschaftliches Bauen im Fels*", Berlin, Springer Verlag (in German).